

# Chapter 1

## Geometric classes

Geometric classes are represents objects in three-dimensional space. These include points, directions, and 3D volumes. Points are implemented as `Eigen::Vector3d` objects (the 3d here means the vector contains 3 `doubles`). Directions are represented by the `UnitVector3d` class, which encapsulates a normalized `Eigen::Vector3d` member. In this section, `Point` is an alias for `Eigen::Vector3d` and `Direction` is an alias for `UnitVector3d`.

3D volumes are derived from the abstract `Shape` class. They must have the following functions overridden in order to be instantiated:

1. `xMin()`, `xMax()`, and so on: locate the extreme points in each of the three Cartesian coordinates.
2. `surfaceArea()`
3. `volume()`
4. `surfaceContains(const Point&)`: checks if the Point is strictly on the surface.
5. `encloses(const Point&)`: checks if the point is strictly inside `*this` (the Shape in question). This means the point is not on the surface or outside.
6. `overlaps(const Shape&)`: checks if the two shapes have a positive volume of intersection. That means if the intersection is a point, a line, or a plane, it returns `false`.
7. `distanceToSurface(const Point&, const Direction&)`: calculates the smallest, positive distance that a point has to travel to reach the surface.
  - If the point is inside the shape, the distance equation will have positive and negative roots, and only the positive root is returned.
  - If the point is on the surface, returns 0 if it leaves the surface, and the distance to the other end if it enters the surface.

- If the point is outside the shape, returns NAN if it never enters the shape, else the smallest distance to the surface.
8. `normal(const Point&)`: checks if the point is on the surface, and returns the outward normal vector if it is.
  9. `print(std::ostream& os)`: outputs the shape into `std::cout`.

`Shape` also has an overloaded `encloses(const Shape&)` that checks if the other shape is completely contained within `*this`. This function evaluates to `true` even if the two `Shapes` intersect on the surface. Because of the tree design, this is made a function within `Shape`, but will always throw an exception unless `*this` is of type `Box`, and practically enclosure check is always done on `Box` objects.

## 1.1 Box

The `Box` class represents an axis-aligned rectangular prism, where its edges align with the axes in Cartesian coordinates. It is defined by a lower vertex  $\mathbf{p}_0$  and upper vertex  $\mathbf{p}_1$ . The edge lengths are  $a = p_{x1} - p_{x0}$ ,  $b = p_{y1} - p_{y0}$ , and  $c = p_{z1} - p_{z0}$ , conventionally called the length, width, and height, respectively.

### 1.1.1 Extreme points

The extreme points are  $p_{x0}$  and  $p_{x1}$  in the x-direction,  $p_{y0}$  and  $p_{y1}$  in y, and  $p_{z0}$  and  $p_{z1}$  in z.

### 1.1.2 Surface area

The surface area is  $2(ab + ac + bc)$ .

### 1.1.3 Volume

The volume is  $abc$ .

### 1.1.4 Checking if a point on the surface

A point  $\mathbf{r}$  is on the one of its six faces if one coordinate is equal to the minimum or maximum coordinate of the box, and the other two coordinates are not outside of their respective extrema. For example, if  $\mathbf{r}$  is on the face defined by  $x = p_{x0}$ , then  $x = p_{x0}$ ,  $p_{y0} \leq y \leq p_{y1}$ , and  $p_{z0} \leq z \leq p_{z1}$ .

### 1.1.5 Checking if a point is inside

A point  $\mathbf{r}$  is inside the box if all coordinates are strictly in between their respective extrema. Mathematically,  $p_{x0} < x < p_{x1}$ ,  $p_{y0} < y < p_{y1}$ , and  $p_{z0} < z < p_{z1}$ .

### 1.1.6 Checking if another volume overlaps

#### Box

Two boxes overlap with for all three coordinates, the maximum value of one box is greater than the minimum value of the other.

#### Sphere

Refer to Section 1.2.6.

#### Ellipsoid

Refer to Section 1.3.6.

### 1.1.7 Distance to surface

Given a point  $\mathbf{r}$  on the box surface with direction  $\hat{\omega}$ , it is travelling away from the box if any of the following conditions is true:

1.  $x = p_{x0}$  and  $\Omega_x \leq 0$ ,
2.  $x = p_{x1}$  and  $\Omega_x \geq 0$ ,
3.  $y = p_{y0}$  and  $\Omega_y \leq 0$ ,
4.  $y = p_{y1}$  and  $\Omega_y \geq 0$ ,
5.  $z = p_{z0}$  and  $\Omega_z \leq 0$ ,
6.  $z = p_{z1}$  and  $\Omega_z \geq 0$ .

The distance to surface should be 0 in these cases according to the function definition.

Otherwise, the distance  $s$  to the plane (not the box face)  $x = p_{x0}$  is

$$s = \frac{x - p_{x0}}{\Omega_x}, \quad (1.1)$$

and similar formulae can be applied to the other planes containing a box face.

Even if negative or undefined values of  $s$  are neglected, the smallest positive value of  $s$  is still not guaranteed to be the distance to the box surface. This is because the calculated  $s$  is the distance to the plane containing a face, not the face itself. An additional check to ensure that after traveling a distance  $s$  to reach a plane, the remaining two coordinates are still in bound. For example, if  $s$  is the distance to the plane  $x = p_{x0}$ , the additional checks are

$$p_{y0} \leq y + \Omega_y s \leq p_{y1} \quad (1.2)$$

$$p_{z0} \leq z + \Omega_z s \leq p_{z1} \quad (1.3)$$

The smallest positive value of  $s$  that also ensures the point is still in bound is the distance to the box surface.

### 1.1.8 Outward normal vector

For a point  $\mathbf{r}$  on the box surface, the normal vector is undefined if  $\mathbf{r}$  lies on a vertex or an edge (the intersection of multiple faces). Otherwise, the normal vector is only dependent on which face the point lies:

1. If  $x = p_{x0}$ ,  $\hat{\mathbf{n}} = -\hat{\mathbf{i}}$
2. If  $x = p_{x1}$ ,  $\hat{\mathbf{n}} = +\hat{\mathbf{i}}$
3. If  $y = p_{y0}$ ,  $\hat{\mathbf{n}} = -\hat{\mathbf{j}}$
4. If  $y = p_{y1}$ ,  $\hat{\mathbf{n}} = +\hat{\mathbf{j}}$
5. If  $z = p_{z0}$ ,  $\hat{\mathbf{n}} = -\hat{\mathbf{k}}$
6. If  $z = p_{z1}$ ,  $\hat{\mathbf{n}} = +\hat{\mathbf{k}}$

### 1.1.9 Checking if another volume is inside

This function is only defined for the `Box` class, which will be useful in a few tree functions. Given a volume with calculated extreme points  $\mathbf{r}_0$  and  $\mathbf{r}_1$ , respectively, the box will completely enclose this volume if the following 6 conditions are true

1.  $p_{x0} \leq x0$
2.  $p_{y0} \leq y0$
3.  $p_{z0} \leq z0$
4.  $p_{x1} \geq x1$
5.  $p_{y1} \geq y1$
6.  $p_{z1} \geq z1$

## 1.2 Sphere

The `Sphere` class requires information of the center,  $\mathbf{r}_0 = [x_0, y_0, z_0]^T$  and of the radius  $R$ . In Cartesian coordinates, the sphere surface is described by the implicit equation:

$$(x - x_0)^2 + (y - y_0)^2 + (z - z_0)^2 = R^2, \quad (1.4)$$

or in vector terms,

$$\|\mathbf{r} - \mathbf{r}_0\|^2 = R^2. \quad (1.5)$$

### 1.2.1 Extreme points

The  $x$ -extrema are  $x_0 \pm R$ , the  $y$ -extrema are  $y_0 \pm R$ , and  $x$ -extrema are  $z_0 \pm R$ .

### 1.2.2 Surface area

The surface area is  $4\pi R^2$ .

### 1.2.3 Volume

The volume is  $\frac{4}{3}\pi R^3$ .

### 1.2.4 Checking if a point on the surface

A point with coordinates  $\mathbf{r}$  is on the sphere surface if it satisfies Equation 1.5.

### 1.2.5 Checking if a point is inside

A point with coordinates  $\mathbf{r}$  is inside the sphere if  $\|\mathbf{r} - \mathbf{r}_0\|^2 < R^2$ .

### 1.2.6 Checking if another volume overlaps

#### Sphere

If the other sphere is centered at  $\mathbf{r}_1$  and has radius  $R_1$ , then it intersects with the current sphere if

$$\|\mathbf{r}_0 - \mathbf{r}_1\| < R + R_1, \quad (1.6)$$

in other words, the two spheres intersect if the line joining their centers is shorter than the sum of the two radii.

#### Box

A box with lower vertex  $\mathbf{p}_0 = [p_{x0}, p_{y0}, p_{z0}]^T$  and upper vertex  $\mathbf{p}_1 = [p_{x1}, p_{y1}, p_{z1}]^T$  overlaps with the sphere if

$$\|\mathbf{r}_0 - \mathbf{p}\| < R, \quad (1.7)$$

where  $\mathbf{p}$  is defined as

$$\mathbf{p} = \begin{bmatrix} \max(p_{x0}, \min(x_0, p_{x1})) \\ \max(p_{y0}, \min(y_0, p_{y1})) \\ \max(p_{z0}, \min(z_0, p_{z1})) \end{bmatrix} \quad (1.8)$$

#### Ellipsoid

Refer to Section 1.3.6.

### 1.2.7 Distance to surface

Given a point  $\mathbf{r}$  travelling at direction  $\hat{\omega}$ , the distance  $s$  to the sphere surface satisfies the equation

$$\|\mathbf{r} + \hat{\omega}s - \mathbf{r}_0\|^2 = R^2, \quad (1.9)$$

which is a quadratic equation in  $s$ . It has the explicit form:

$$s^2 + 2Bs + C = 0, \quad (1.10)$$

where the coefficients  $B$  and  $C$  are defined as

$$B = (\mathbf{r} - \mathbf{r}_0) \cdot \hat{\omega} \quad (1.11)$$

$$C = \|\mathbf{r} - \mathbf{r}_0\|^2 - R^2. \quad (1.12)$$

### 1.2.8 Outward normal vector

The outward normal vector of a point  $\mathbf{r}$  on the sphere surface is  $\frac{\mathbf{r} - \mathbf{r}_0}{R}$ .

## 1.3 Ellipsoid

The `Ellipsoid` class represents a shape centered at  $\mathbf{r}_0$ , of which the surface is given as

$$(\mathbf{r} - \mathbf{r}_0) \cdot \mathbf{M}(\mathbf{r} - \mathbf{r}_0) = 1, \quad (1.13)$$

where  $\mathbf{M}$  is a symmetric positive definite (SPD) matrix in  $\mathbb{R}^3$  that holds the orientation and magnitude of the ellipsoid. Its unit eigenvectors – denoted as  $\hat{\mathbf{e}}_0$ ,  $\hat{\mathbf{e}}_1$ , and  $\hat{\mathbf{e}}_2$  – form an orthonormal basis that corresponds to the direction of the three primary axes. The corresponding eigenvalues are the inverse square of the respective semi-axis. In other words, if  $a$ ,  $b$ , and  $c$  are the semi-axes, and  $\lambda_i$  is the  $i^{\text{th}}$  eigenvalue of  $\mathbf{M}$ , then  $\lambda_0 = \frac{1}{a^2}$ ,  $\lambda_1 = \frac{1}{b^2}$ , and  $\lambda_2 = \frac{1}{c^2}$ .

If the three axes are aligned to Cartesian coordinates, then Equation 1.13 can be expanded as

$$\left(\frac{x - x_0}{a}\right)^2 + \left(\frac{y - y_0}{b}\right)^2 + \left(\frac{z - z_0}{c}\right)^2 = 1, \quad (1.14)$$

and the matrix  $\mathbf{M}$  is

$$\mathbf{M} = \begin{bmatrix} \frac{1}{a^2} & 0 & 0 \\ 0 & \frac{1}{b^2} & 0 \\ 0 & 0 & \frac{1}{c^2} \end{bmatrix}. \quad (1.15)$$

Such ellipsoid is called axis-aligned, similar to the `Box` class.

A sphere can also be represented by the `Ellipsoid` class, in which case  $a = b = c = R$ , and  $\mathbf{M} = \frac{1}{R^2} \mathbf{I}$ .

### 1.3.1 Extreme points

This is a constrained optimization problem. Take the  $x$  coordinate for example, the problem is to maximize or minimize  $f(\mathbf{r}) = x = \hat{\mathbf{i}} \cdot \mathbf{r}$  subject to the constraint in Equation 1.13, i.e.  $g(\mathbf{r}) = (\mathbf{r} - \mathbf{r}_0) \cdot \mathbf{M}(\mathbf{r} - \mathbf{r}_0) = 1$ . This problem is solvable through the Lagrange multipliers method, where  $\nabla f$  and  $\nabla g$  are required:

$$\nabla f(\mathbf{r}) = \hat{\mathbf{i}} \quad (1.16)$$

$$\nabla g(\mathbf{r}) = 2\mathbf{M}(\mathbf{r} - \mathbf{r}_0). \quad (1.17)$$

The following a system of 4 equations is formulated to solve for  $\mathbf{r}$  and  $\lambda$ :

$$\begin{aligned} 2\lambda\mathbf{M}(\mathbf{r} - \mathbf{r}_0) &= \hat{\mathbf{i}} \\ g(\mathbf{r}) &= 1. \end{aligned} \quad (1.18)$$

Equation 1.18 is used to solve for  $\mathbf{r}$  in terms of  $\lambda$ :

$$\mathbf{r} = \mathbf{r}_0 + \frac{1}{2\lambda}\mathbf{M}^{-1}\hat{\mathbf{i}}, \quad (1.19)$$

and this expression can be substituted back to the constraint in Equation 1.13 to solve for  $\lambda$ :

$$\frac{1}{2\lambda}\mathbf{M}^{-1}\hat{\mathbf{i}} \cdot \frac{1}{2\lambda}\mathbf{M}\mathbf{M}^{-1}\hat{\mathbf{i}} = 1 \quad (1.20)$$

$$\frac{1}{4\lambda^2}\hat{\mathbf{i}} \cdot \mathbf{M}^{-1}\hat{\mathbf{i}} = 1 \quad (1.21)$$

$$\lambda = \frac{\pm 1}{2}\sqrt{\hat{\mathbf{i}} \cdot \mathbf{M}^{-1}\hat{\mathbf{i}}}. \quad (1.22)$$

There are two possible values for  $\lambda$ , as expected, as the minimum and maximum  $x$  points are collinear with the ellipsoid center. Substituting the expression for  $\lambda$  in Equation 1.22 back to Equation 1.19 to obtain

$$\mathbf{r} = \mathbf{r}_0 \pm \frac{\mathbf{M}^{-1}\hat{\mathbf{i}}}{\sqrt{\hat{\mathbf{i}} \cdot \mathbf{M}^{-1}\hat{\mathbf{i}}}}, \quad (1.23)$$

the objective function  $f(\mathbf{r}) = \hat{\mathbf{i}} \cdot \mathbf{r}$  can finally be optimized:

$$x = \hat{\mathbf{i}} \cdot \mathbf{r} = x_0 \pm \sqrt{\hat{\mathbf{i}} \cdot \mathbf{M}^{-1}\hat{\mathbf{i}}} \quad (1.24)$$

Since  $\mathbf{M}$  is required to be SPD, its inverse can be easily computed. The eigendecomposition of  $\mathbf{M}$ , which has to be carried out regardless in order to obtain the principal axes and their respective length, is

$$\mathbf{M} = \mathbf{E}\Lambda\mathbf{E}^T, \quad (1.25)$$

and from there the inverse matrix  $\mathbf{M}^{-1}$  is

$$\mathbf{M}^{-1} = \mathbf{E}\Lambda^{-1}\mathbf{E}^T, \quad (1.26)$$

where  $\boldsymbol{\Lambda}^{-1}$  is a diagonal matrix whose entries are the reciprocal of those in  $\boldsymbol{\Lambda}$ . In terms of the semi-axes, the entries of  $\boldsymbol{\Lambda}^{-1}$  are  $a^2$ ,  $b^2$ , and  $c^2$ .

For the purpose of finding the extreme points, the entire inverse matrix is not needed. Note that  $\hat{\mathbf{i}} \cdot \mathbf{M}^{-1} \hat{\mathbf{i}}$  is simply the first-row, first-column entry of  $M^{-1}$ . Using the decomposition in Equation 1.26, this entry can be obtained by:

$$\begin{aligned}\hat{\mathbf{i}} \cdot \mathbf{M}^{-1} \hat{\mathbf{i}} &= \hat{\mathbf{i}} \cdot \mathbf{E}^T \boldsymbol{\Lambda}^{-1} \mathbf{E} \hat{\mathbf{i}} \\ &= (\mathbf{E}^T \hat{\mathbf{i}}) \cdot \boldsymbol{\Lambda}^{-1} \mathbf{E}^T \hat{\mathbf{i}} \\ &= a^2 E_{0,0}^2 + b^2 E_{0,1}^2 + c^2 E_{0,2}^2\end{aligned}$$

Similar approaches can be carried out to find the minima and maxima in the other coordinates. The results are as follows:

$$x_{\min/\max} = x_0 \pm \sqrt{a^2 E_{0,0}^2 + b^2 E_{0,1}^2 + c^2 E_{0,2}^2} \quad (1.27)$$

$$y_{\min/\max} = y_0 \pm \sqrt{a^2 E_{1,0}^2 + b^2 E_{1,1}^2 + c^2 E_{1,2}^2} \quad (1.28)$$

$$z_{\min/\max} = z_0 \pm \sqrt{a^2 E_{2,0}^2 + b^2 E_{2,1}^2 + c^2 E_{2,2}^2} \quad (1.29)$$

For an axis-aligned ellipsoid, since  $E_{i,j} = \delta_{i,j}$ , Equations 1.27 through 1.29 do simplify to  $x_0 \pm a$ ,  $y_0 \pm b$ , and  $z_0 \pm c$ , respectively.

### 1.3.2 Surface area

There are no analytic forms of an ellipsoid surface area; it generally involves computing elliptic integrals. The exact formulation is given in [3]:

$$S = 2\pi c^2 + \frac{2\pi ab}{\sqrt{\delta}} \left[ (1-\delta)F\left(\sqrt{\delta} \left| \frac{\epsilon}{\delta}\right.\right) + \delta E\left(\sqrt{\delta} \left| \frac{\epsilon}{\delta}\right.\right) \right], \quad (1.30)$$

where  $F(x|k)$  and  $E(x|k)$  are the incomplete elliptic integrals of the first and second kind, respectively. The parameters  $\delta$  and  $\epsilon$  are defined assuming that  $c \leq b \leq a$ :

$$\delta = 1 - \frac{c^2}{a^2} \quad (1.31)$$

$$\epsilon = 1 - \frac{c^2}{b^2}. \quad (1.32)$$

The elliptical integrals are undefined when  $a = b = c$ , since both  $\epsilon$  and  $\delta$  are in an indeterminate form. Obviously the spherical case is a useful benchmark, so a different integral has to be derived.

The surface of an ellipsoid octant where all coordinates are non-negative can be parametrized as

$$\begin{aligned}\mathbf{r}(u, v) &= a\sqrt{1-u^2} \cos(v)\hat{\mathbf{e}}_0 + b\sqrt{1-u^2} \sin(v)\hat{\mathbf{e}}_1 + cu\hat{\mathbf{e}}_2 \\ 0 \leq u &\leq 1, 0 \leq v \leq \frac{\pi}{2}.\end{aligned}$$

Using these parametrizations, the surface area of the entire ellipsoid (which is 8 times that of an octant) can be computed as

$$S = 8abc \int_0^{\frac{\pi}{2}} \int_0^1 \sqrt{\frac{(1-u^2)\cos^2(v)}{a^2} + \frac{(1-u^2)\sin^2(v)}{b^2} + \frac{u^2}{c^2}} du dv \quad (1.33)$$

### 1.3.3 Volume

The volume is  $\frac{4}{3}\pi abc$ .

### 1.3.4 Checking if a point on the surface

A point with coordinates  $\mathbf{r} = [x, y, z]^T$  is on the ellipsoid surface if it satisfies Equation 1.13. For an axis-aligned ellipsoid, Equation 1.13 is simplified to Equation 1.14.

### 1.3.5 Checking if a point is inside

A point with coordinates  $\mathbf{r}$  is inside the ellipsoid if it satisfies the inequality

$$(\mathbf{r} - \mathbf{r}_0) \cdot \mathbf{M}(\mathbf{r} - \mathbf{r}_0) < 1.$$

The case of an axis-aligned ellipsoid is defined similarly.

### 1.3.6 Checking if another volume overlaps

#### Ellipsoid and sphere

The collision detection test between two ellipsoids (which can also extend to spheres) is implemented from the algorithm proposed by Gilitschenski [2], with a minor modification (see below). Let  $\Delta\mathbf{r}$  be the vector connecting the two centers, and  $\mathbf{A}$  and  $\mathbf{B}$  be the matrices that define the two ellipsoids. A convex function  $K(\lambda) : (0, 1) \rightarrow \mathbb{R}$  can be defined as

$$K(\lambda) = 1 - \Delta\mathbf{r} \cdot \left( \frac{1}{\lambda} \mathbf{A}^{-1} + \frac{1}{1-\lambda} \mathbf{B}^{-1} \right)^{-1} \Delta\mathbf{r}. \quad (1.34)$$

The two ellipsoids are non-overlapping if there exists a  $\lambda \in (0, 1)$  such that  $K(\lambda) \leq 0$ . Because of the convexity, it also means that  $\min K(\lambda) \leq 0$ . In the special case of  $\min K(\lambda) = 0$ , the region of intersection is a single point, and the two shapes are also considered non-overlapping per the definition of this function. Instead of finding where  $\min K$  occurs, this problem is approached as a root-solving problem.

Gilitschenski proposes that instead of finding what the minimum is, a root-finding problem can be used to find if  $K(\lambda)$  has two distinct real roots on the interval  $(0, 1)$  [2]. This is equivalent to  $\min K(\lambda) \leq 0$ , since  $K(\lambda)$  is a convex function on  $(0, 1)$ . The algorithm implemented in this code involves finding

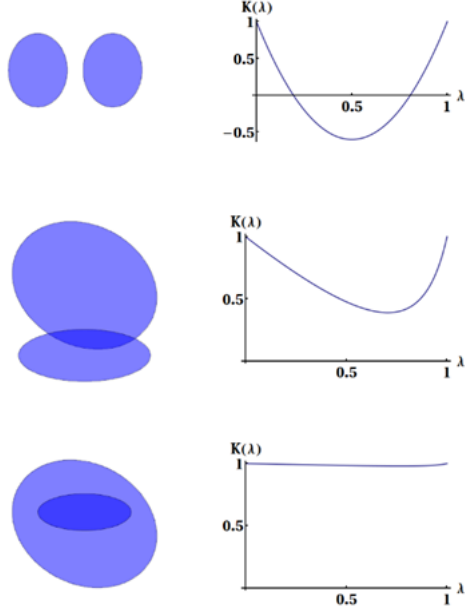


Figure 1.1: Ellipsoid collision test demonstrated  $K(\lambda)$  plotted on the right. It can be seen that the two ellipsoids are non-overlapping if and only if  $\min K(\lambda) \leq 0$ . Figure from [2].

only one of two possible roots, called  $\lambda_0$ , and if it is found, the two ellipsoids do not overlap. This is also true for the special case of a double root, since the intersection is a single point and the two ellipsoids are still considered non-overlapping.

### Box

The collision detection test between an ellipsoid and a box is implemented from the algorithm proposed by Eberly [1]; however, the edge and face tests described below are slightly modified. The main idea is still to check whether the ellipsoid intersects with the box centroid, if not then any of its vertices, then any of its edges, and finally any of its faces. The point checks can be referred back to Section 1.3.5.

An edge can be represented parametrically by its two endpoints  $\mathbf{r}_0$  and  $\mathbf{r}_1$  through the equation  $\mathbf{e}(t) = \mathbf{p}_0 + (\mathbf{p}_1 - \mathbf{p}_0)t$  for  $t \in [0, 1]$ . Define  $K(t)$  as

$$K(t) = (\mathbf{e}(t) - \mathbf{r}_0) \cdot \mathbf{M}(\mathbf{e}(t) - \mathbf{r}_0), \quad (1.35)$$

which expands into

$$K(t) = At^2 + 2Bt + C, \quad (1.36)$$

where

$$A = (\mathbf{p}_1 - \mathbf{p}_0) \cdot \mathbf{M}(\mathbf{p}_1 - \mathbf{p}_0) \quad (1.37)$$

$$B = (\mathbf{p}_1 - \mathbf{p}_0) \cdot \mathbf{M}(\mathbf{p}_0 - \mathbf{r}_0) \quad (1.38)$$

$$C = (\mathbf{p}_0 - \mathbf{r}_0) \cdot \mathbf{M}(\mathbf{p}_0 - \mathbf{r}_0). \quad (1.39)$$

Since  $\mathbf{p}_0$  and  $\mathbf{p}_1$  are both outside the ellipsoid (otherwise this test would not be needed),  $K(0) > 1$  and  $K(1) > 1$ . If  $\mathbf{e}(t)$  does intersect the ellipsoid, and is not just tangential to it, there also must exist a  $t$  where  $K(t) < 1$ , and by the Intermediate Value Theorem, the intersections exist and satisfy  $K(t) = 1$ . In fact, the minimum value of  $K(t)$  must be less than 1 in order for the edge to intersect the ellipsoid. This optimization problem is easy to solve for since the function of interest is quadratic. The derivative is given by:

$$\frac{1}{2} \frac{dK}{dt} = At + B = 0. \quad (1.40)$$

It is worth noting that the second derivative of  $K(t) - 2A$  – is strictly positive since  $\mathbf{M}$  is an SPD matrix. Therefore,  $K(t)$  has a global minimum at the critical point  $t = \frac{-B}{A}$ ,  $K(t)$ . It is also important to check that this critical point is bounded by the domain  $[0, 1]$ .

In summary, the conditions for an edge to intersect the ellipsoid are as follows

$$-1 \leq \frac{B}{A} \leq 0 \quad (1.41)$$

$$K\left(\frac{-B}{A}\right) < 1 \quad (1.42)$$

Similarly, a face can be defined by three of its four endpoints  $\mathbf{p}_0$ ,  $\mathbf{p}_1$ , and  $\mathbf{p}_2$ , where  $(\mathbf{p}_1 - \mathbf{p}_0) \cdot (\mathbf{p}_2 - \mathbf{p}_0) = 0$ . The parametric equation for a face is

$$\begin{aligned} \mathbf{f}(u, v) &= \mathbf{p}_0 + (\mathbf{p}_1 - \mathbf{p}_0)u + (\mathbf{p}_2 - \mathbf{p}_0)v \\ (u, v) &\in [0, 1]^2. \end{aligned}$$

Define

$$K(u, v) = (\mathbf{f}(u, v) - \mathbf{r}_0) \cdot \mathbf{M}(\mathbf{f}(u, v) - \mathbf{r}_0), \quad (1.43)$$

which expands into

$$K(u, v) = Au^2 + 2Buv + Cv^2 + 2Du + 2Ev + F, \quad (1.44)$$

where

$$A = (\mathbf{p}_1 - \mathbf{p}_0) \cdot \mathbf{M}(\mathbf{p}_1 - \mathbf{p}_0) \quad (1.45)$$

$$B = (\mathbf{p}_1 - \mathbf{p}_0) \cdot \mathbf{M}(\mathbf{p}_2 - \mathbf{p}_0) \quad (1.46)$$

$$C = (\mathbf{p}_2 - \mathbf{p}_0) \cdot \mathbf{M}(\mathbf{p}_2 - \mathbf{p}_0) \quad (1.47)$$

$$D = (\mathbf{p}_1 - \mathbf{p}_0) \cdot \mathbf{M}(\mathbf{p}_0 - \mathbf{r}_0) \quad (1.48)$$

$$E = (\mathbf{p}_2 - \mathbf{p}_0) \cdot \mathbf{M}(\mathbf{p}_0 - \mathbf{r}_0) \quad (1.49)$$

$$F = (\mathbf{p}_0 - \mathbf{r}_0) \cdot \mathbf{M}(\mathbf{p}_0 - \mathbf{r}_0). \quad (1.50)$$

$K(u, v)$  is minimized if

$$\frac{1}{2} \nabla K = \begin{bmatrix} A & B \\ B & C \end{bmatrix} \begin{bmatrix} u \\ v \end{bmatrix} + \begin{bmatrix} D \\ E \end{bmatrix} = \mathbf{0}, \quad (1.51)$$

which occurs at

$$\begin{aligned} \begin{bmatrix} u \\ v \end{bmatrix} &= - \begin{bmatrix} A & B \\ B & C \end{bmatrix}^{-1} \begin{bmatrix} D \\ E \end{bmatrix} \\ \begin{bmatrix} u \\ v \end{bmatrix} &= \frac{1}{B^2 - AC} \begin{bmatrix} C & -B \\ -B & A \end{bmatrix} \begin{bmatrix} D \\ E \end{bmatrix} \\ \begin{bmatrix} u \\ v \end{bmatrix} &= \frac{1}{B^2 - AC} \begin{bmatrix} CD - BE \\ AE - BD \end{bmatrix} \end{aligned} \quad (1.52)$$

Therefore, the conditions for a face to intersect the ellipsoid are as follows

$$B^2 - AC \neq 0 \quad (1.53)$$

$$0 \leq \frac{CD - BE}{B^2 - AC} \leq 1 \quad (1.54)$$

$$0 \leq \frac{AE - BD}{B^2 - AC} \leq 1 \quad (1.55)$$

$$K \left( \frac{CD - BE}{B^2 - AC}, \frac{AE - BD}{B^2 - AC} \right) < 1 \quad (1.56)$$

If a box does not overlap with the ellipsoid, it has undergone the centroid containment test, 8 vertex containment tests, 12 edge overlap tests, and 6 face overlap tests. Eberly proposes a closest-features testing

### 1.3.7 Distance to surface

Given a point  $\mathbf{r}$  travelling at direction  $\hat{\omega}$ , the distance  $s$  to surface of the ellipsoid satisfies the equation

$$(\mathbf{r} + \hat{\omega}s - \mathbf{r}_0) \cdot \mathbf{M} (\mathbf{r} + \hat{\omega}s - \mathbf{r}_0) = 1. \quad (1.57)$$

Equation 1.57 can be written in a quadratic form in  $s$ :

$$As^2 + 2Bs + C = 0, \quad (1.58)$$

where the coefficients  $A$ ,  $B$  and  $C$  are defined as

$$A = \hat{\omega} \cdot \mathbf{M} \hat{\omega} \quad (1.59)$$

$$B = \hat{\omega} \cdot \mathbf{M} (\mathbf{r} - \mathbf{r}_0) \quad (1.60)$$

$$C = (\mathbf{r} - \mathbf{r}_0) \cdot \mathbf{M} (\mathbf{r} - \mathbf{r}_0) - 1. \quad (1.61)$$

### 1.3.8 Outward normal vector

Given the explicit form  $f(\mathbf{r}) = (\mathbf{r} - \mathbf{r}_0) \cdot \mathbf{M}(\mathbf{r} - \mathbf{r}_0)$ , the normal vector at a point  $\mathbf{r}$  on the surface is parallel to  $\nabla f(\mathbf{r})$ . Therefore,

$$\hat{\mathbf{n}}(\mathbf{r}) = \frac{\nabla f(\mathbf{r})}{\|\nabla f(\mathbf{r})\|} = \frac{\mathbf{M}(\mathbf{r} - \mathbf{r}_0)}{\|\mathbf{M}(\mathbf{r} - \mathbf{r}_0)\|} \quad (1.62)$$

For an axis-aligned ellipsoid, Equation 1.62 simplifies to:

$$\hat{\mathbf{n}}(\mathbf{r}) = \frac{1}{\sqrt{\left(\frac{x-x_0}{a^2}\right)^2 + \left(\frac{y-y_0}{b^2}\right)^2 + \left(\frac{z-z_0}{c^2}\right)^2}} \left[ \frac{x-x_0}{a^2} \hat{\mathbf{i}} + \frac{y-y_0}{b^2} \hat{\mathbf{j}} + \frac{z-z_0}{c^2} \hat{\mathbf{k}} \right] \quad (1.63)$$

## 1.4 Shape defined by a closed parametric surface

A parametric surface is described by a function  $\mathbf{r}(u, v) : \mathbb{R}^2 \rightarrow \mathbb{R}^3 = x(u, v)\hat{\mathbf{i}} + y(u, v)\hat{\mathbf{j}} + z(u, v)\hat{\mathbf{k}}$ , defined over  $u \in [u_0, u_1]$  and  $v \in [v_0, v_1]$ . It is assumed that  $\mathbf{r}(u, v)$  is of class  $C^2$ , so the partial derivatives  $\mathbf{r}_u = \frac{\partial \mathbf{r}}{\partial u}$ ,  $\mathbf{r}_v = \frac{\partial \mathbf{r}}{\partial v}$ ,  $\mathbf{H}_x = \nabla \otimes \nabla x$ ,  $\mathbf{H}_y = \nabla \otimes \nabla y$ , and  $\mathbf{H}_z = \nabla \otimes \nabla z$  exist. They can be provided by the user or calculated numerically.

Because of the extensive use of derivative and integral operators, repeatedly calculating some properties of similar shapes can be expensive. All parametric surfaces have shared pointer to a common base shape  $\mathbf{r}(u, v)$ , provided that they are defined by a set related parametric equations  $\mathbf{r}'(u, v) = \mathbf{M}\mathbf{r}(u, v) + \mathbf{r}_0$ , where  $\mathbf{M}$  is an invertible linear transformation matrix in  $\mathbb{R}^{3 \times 3}$ , and  $\mathbf{r}_0$  is a translation vector.

### 1.4.1 Extreme points

Determining the extreme points in any Cartesian direction is a constrained optimization problem, since they must occur at either at the boundary or a critical point within. Take the x-coordinate of a base parametric surface for example, this involves locating the global minimum of  $x(u, v)$  on the box interval  $[u_0, u_1] \times [v_0, v_1]$ .

Because of the low dimensionality of the functions (2), computing the Hessian (of  $x(u, v)$ , for example) is cheap. The method of choice is the projected Newton's method. Similar to the Levenberg–Marquardt least-square algorithm, an addition of  $\alpha \mathbf{I}$  (for an  $\alpha \geq 0$ ) to the Hessian may be needed to ensure that it is positive definite. At every iteration, a backtracking line search along the search direction  $(\mathbf{H} + \alpha \mathbf{I})^{-1} \nabla x$  is needed to ensure that the solution stays constrained while satisfying the Armijo condition.

For a transformed shape, the x-component and its derivative functions are given as

$$x'(u, v) = \mathbf{M}_0 \mathbf{r}(u, v) + x_0 \quad (1.64)$$

$$(\nabla x')^T = \mathbf{M}_0 [\mathbf{r}_u \quad \mathbf{r}_v] \quad (1.65)$$

$$\mathbf{H}_{x'} = M_{00} \mathbf{H}_x + M_{01} \mathbf{H}_y + M_{02} \mathbf{H}_z \quad (1.66)$$

where  $\mathbf{M}_0$  is the row vector corresponding to the first row of  $\mathbf{M}$ .

If  $\mathbf{M}$  is a scaling matrix that scales the x-coordinate by a scalar  $k_x$ , then the extrema points of  $x'$  are  $x'_{\min} = k_x x_{\min} + x_0$  and  $x'_{\max} = k_x x_{\max} + x_0$ .

Similar procedures can be followed for the y and z coordinates.

### 1.4.2 Surface area

The surface area of a base parametric surface is

$$S = \int_{v_0}^{v_1} \int_{u_0}^{u_1} \|\mathbf{r}_u \times \mathbf{r}_v\| dudv. \quad (1.67)$$

Rotation and reflection do not alter the surface area. Uniform scaling by a scalar  $K$  scales the surface area by  $K^2$ . Any other transformation will require a re-evaluation of the integral in Equation 1.67 as

$$S = \int_{v_0}^{v_1} \int_{u_0}^{u_1} \|\mathbf{M} \mathbf{r}_u \times \mathbf{M} \mathbf{r}_v\| dudv. \quad (1.68)$$

### 1.4.3 Volume

The volume is only defined for a closed surface, since we can take advantage of the Divergence Theorem

$$\iiint_{\Gamma} (\nabla \cdot \mathbf{F}) dV = \oint_{\partial\Gamma} \mathbf{F} \cdot d\mathbf{S}. \quad (1.69)$$

Rather than integrating over a volume, the better alternative is to find an  $\mathbf{F}$  such that  $\nabla \cdot \mathbf{F} = 1$  and integrate it over the surface. From Equation 1.67, if we follow the convention

$$S = \oint_{\partial\Gamma} d\mathbf{S} = \oint_{\partial\Gamma} \hat{\mathbf{n}} \cdot d\mathbf{S}, \quad (1.70)$$

the unit normal vector  $\hat{\mathbf{n}}$  and the differential surface area  $d\mathbf{S}$  can be defined as

$$\hat{\mathbf{n}} \equiv \frac{\mathbf{r}_u \times \mathbf{r}_v}{\|\mathbf{r}_u \times \mathbf{r}_v\|} \quad (1.71)$$

$$d\mathbf{S} \equiv (\mathbf{r}_u \times \mathbf{r}_v) dudv. \quad (1.72)$$

The last task to find a function  $\mathbf{F}$  such that  $\nabla \cdot \mathbf{F} = 1$ . The most obvious candidates are  $\mathbf{F} = x\hat{\mathbf{i}}$ ,  $\mathbf{F} = y\hat{\mathbf{j}}$ , and  $\mathbf{F} = z\hat{\mathbf{k}}$ . Choosing the last candidate, the expression for the volume is:

$$\begin{aligned} V &= \int_{v_0}^{v_1} \int_{u_0}^{u_1} z\hat{\mathbf{k}} \cdot (\mathbf{r}_u \times \mathbf{r}_v) dudv \\ &= \int_{v_0}^{v_1} \int_{u_0}^{u_1} z \left( \frac{\partial x}{\partial u} \frac{\partial y}{\partial v} - \frac{\partial x}{\partial v} \frac{\partial y}{\partial u} \right) dudv. \end{aligned} \quad (1.73)$$

The volume of a transformed shape is that of the base shape scaled by  $|\det \mathbf{M}|$ .

#### 1.4.4 Checking if a point on the surface

A point  $\mathbf{p}$  is on the parametric surface  $\mathbf{r}(u, v)$  (regardless of if it's a base or transformed surface) if there exists a pair  $(u, v)$  that satisfies the system of equation

$$\mathbf{p} - \mathbf{r}(u, v) = \mathbf{0}. \quad (1.74)$$

This is a non-linear least square problem, since the system has 3 equations but only 2 unknowns. Given the least-square solution  $(u^*, v^*)$  to Equation 1.74, then  $\mathbf{p}$  is on the parametric surface if

$$\|\mathbf{p} - \mathbf{r}(u^*, v^*)\| = 0. \quad (1.75)$$

In other words,  $(u^*, v^*)$  has to satisfy Equation 1.74 exactly (or within a numerical tolerance) rather than merely minimizing the residual.

#### 1.4.5 Checking if a point is inside

The concept of "inside" (and by extension "outside") is only well-defined if the surface is closed. For simplicity, the surface is assumed convex. A point  $\mathbf{p}$  is inside the volume enclosed by the parametric surface if regardless of the direction at which it travels, there is a positive distance to the surface. This problem reduces to two distance calculation problems, one with a direction  $\hat{\omega}$  and the other with  $-\hat{\omega}$ , and checking whether both distances are positive. The choice of  $\hat{\omega}$  is arbitrary. Refer to section 1.4.7 for the actual distance calculation.

#### 1.4.6 Checking if another volume overlaps

#### 1.4.7 Distance to surface

Given a point  $\mathbf{p}$  travelling at direction  $\hat{\omega}$ , the distance  $s$  to surface of the sphere satisfies the equation

$$\mathbf{p} + \hat{\omega}s = \mathbf{M}\mathbf{r}(u, v) + \mathbf{r}_0.$$

This can be arranged into an objective function of three variables:

$$\mathbf{F}(u, v, s) = \mathbf{p}_0 + \hat{\omega}s - \mathbf{M}\mathbf{r}(u, v) - \mathbf{r}_0, \quad (1.76)$$

and the goal is to solve for the solution vector  $\mathbf{s} = [u, v, s]^T$  such that  $\mathbf{F}(\mathbf{s}) = \mathbf{0}$ .

Since the Jacobian of  $\mathbf{F}$  is known

$$\mathbf{J} = [-M\mathbf{r}_u \quad -M\mathbf{r}_v \quad \hat{\boldsymbol{\omega}}], \quad (1.77)$$

Newton's method can be used to solve for  $\mathbf{s}$ . The solution is permissible if  $u$  and  $v$  are both in bound, and  $s \geq 0$ .

#### 1.4.8 Outward normal vector

The outward normal vector is defined in Equation 1.71.

### 1.5 Shape defined by an implicit function

# Chapter 2

## Tree classes

The motive for using a Tree data structure is to quickly locate which —Shape— object (potentially out of thousands or millions) that a ray of photon will enter next, which is our version of the nearest neighbor search algorithm. A brute-force approach will have a time-complexity of order  $\mathcal{O}(N)$ , which in itself is not ideal. Furthermore, distance calculations are expensive because of the use of the square-root function (in case of the `Sphere` class) or some other functions that are potentially more expensive. A tree is a hierarchical data structure that groups objects based on certain common features. In this case, an Octree is used to group 3D shapes into each of the 8 octants of equal volume. Using a tree structure, the average time-complexity is down to  $\mathcal{O}(\log N)$ , which scales extremely well for large datasets. The majority of distance calculations involving those octants are to a surface of a box, and therefore are linear in nature, leaving a very few expensive calculations at the end.

### BoundingBox

The `BoundingBox` class is derived from `Box` and represents an axis-aligned bounding box (AABB). It is the building block of an `Octree` and therefore is constrained to have at most 8 children. A `Node` is defined as a pointer to a `Shape` - more specifically, a `std::unique_ptr<Shape>` - that is contained within a `BoundingBox`. The pointed-to `Shape` itself can be either another `BoundingBox` (which means there are further subdivisions within that particular octant) or a terminal shape (which means they are leaf nodes).

### Octree

## Chapter 3

# Propogation of light in matter

Light is a manifestation of travelling electric and magnetic field. The two fields oscillate perpendicular to each other and to the direction at which light travels. They both have wavenumber  $k$  and frequency  $\omega$ . Let  $x$  be the direction of propagation of the eletric field, the field can be expressed as

$$\mathbf{E}(x, t) = \mathbf{E}_0 \Re \left[ e^{i(kx - \omega t)} \right] \quad (3.1)$$

To be precise, the term "wavenumber" refers to the angular wavenumber and is defined as the number of radians per unit length. In a vacuum with no attenuation, it is related to the phase velocity  $v_p$  as

$$k = \frac{\omega}{v_p}. \quad (3.2)$$

Since the phase velocity is a fraction  $n$  lower than the speed of light in vacuum  $c$ , the relation between wavenumber and refractive index is

$$k = \frac{\omega n}{c} \quad (3.3)$$

In an unattenuated medium,  $k$  is a real number, and the variable  $n$  is known as the refractive index. This only holds in vacuum; in any other material,  $k$  is a complex number, with its imaginary part accounting for the extent of attenuation.  $n$  therefore must also be a complex number. From now on, the variable  $n$  refers the real part of  $n + i\kappa$ , and the imaginary part  $\kappa$  is called the extinction coefficient. In other words,

$$k = \frac{\omega}{c} (n + i\kappa) \quad (3.4)$$

To show that attenuation is accounted for by the imaginary component, Equation 3.1 can be expanded as

$$\begin{aligned}\mathbf{E}(x, t) &= \mathbf{E}_0 \Re \left[ \exp \left[ -\frac{\omega}{c} \kappa x + i \left( \frac{\omega}{c} n x - \omega t \right) \right] \right] \\ &= \mathbf{E}_0 \exp \left( -\frac{\omega}{c} \kappa x \right) \cos \left( \frac{\omega}{c} n x - \omega t \right)\end{aligned}\quad (3.5)$$

Here, the electric field strength falls off exponentially with distance travelled, and the decay extent is characterized by the extinction coefficient. This resembles the linear attenuation of light intensity

$$I(x) = I_0 e^{-\sigma x}, \quad (3.6)$$

and the two equations are in fact related. Since the medium of interest is non-magnetic,  $\mathbf{B} \approx \mu \mathbf{H}$ , and the magnetic permeability  $\mu$  can be readily approximated as its vacuum value  $\mu_0 = 4\pi \times 10^{-7}$  H/m. The Poynting vector, defined as

$$\mathbf{S} \equiv \mathbf{E} \times \mathbf{H}, \quad (3.7)$$

can be written in terms of the  $\mathbf{B}$  field:

$$\mathbf{S} = \frac{1}{\mu} \mathbf{E} \times \mathbf{B}. \quad (3.8)$$

Thanks to Maxwell's Equations, the  $\mathbf{E}$  and  $\mathbf{B}$  are in phase in both spatial and temporal domains. In terms of magnitude, the two fields are proportional by a factor of  $c/n$ , or the wave speed. As a result,

$$\mathbf{S}(x, t) = \frac{n}{\mu c} \|\mathbf{E}_0\|^2 \exp \left( -\frac{2\omega}{c} \kappa x \right) \cos^2 \left( \frac{\omega}{c} n x - \omega t \right) \hat{\mathbf{x}}. \quad (3.9)$$

The light intensity is defined as the time-averaged magnitude of the Poynting vector:

$$I(x) = \langle \|\mathbf{S}(x, t)\| \rangle \quad (3.10)$$

$$= \frac{n}{\mu c} \|\mathbf{E}_0\|^2 \exp \left[ -\frac{2\omega}{c} \kappa x \right] \cdot \frac{1}{T} \int_0^T \cos^2 \left( \frac{\omega}{c} n x - \omega t \right) dt. \quad (3.11)$$

Assume the integrating time  $T$  is much larger than the wave period - i.e.  $T \gg \frac{2\pi}{\omega}$ , then the averaging integral in Equation 3.11 will approach the average value over one single period, which is  $\frac{1}{2}$ . Therefore,

$$I(x) = \frac{n}{2\mu c} \|\mathbf{E}_0\|^2 \exp \left[ -\frac{2\omega}{c} \kappa x \right]. \quad (3.12)$$

The relation between the attenuation coefficient  $\sigma$  and the extinction coefficient  $\kappa$  is then

$$\boxed{\sigma = \frac{2\omega\kappa}{c}}.$$

(3.13)

## Chapter 4

# Snell's Law and Orientation of the Transmitted Ray

Let  $\hat{\mathbf{i}}$  be the incident vector,  $\hat{\mathbf{n}}$  be the (outward) normal vector, and  $\hat{\mathbf{t}}$  be the transmitted vector. Also the index of refraction of a medium is labeled  $n$ .

Our job is to find  $\hat{\mathbf{t}}$ , given  $\hat{\mathbf{i}}$ ,  $\hat{\mathbf{n}}$ ,  $n_1$  and  $n_2$ . The vectors are related through Snell's Law, and in vector notation it reads

$$n_1 (\hat{\mathbf{i}} \times \hat{\mathbf{n}}) = n_2 (\hat{\mathbf{t}} \times \hat{\mathbf{n}}), \quad (4.1)$$

or

$$\hat{\mathbf{t}} \times \hat{\mathbf{n}} = \mathbf{c}, \quad (4.2)$$

for the new vector  $\mathbf{c}$  defined as  $\mathbf{c} = \frac{n_1}{n_2} (\hat{\mathbf{i}} \times \hat{\mathbf{n}})$ . Note that  $\mathbf{c}$  and  $\hat{\mathbf{n}}$  are orthogonal.

We start solving for  $\hat{\mathbf{t}}$  by decomposing it into two components: one parallel and one orthogonal to  $\hat{\mathbf{n}}$ :

$$\hat{\mathbf{t}} = t_{\parallel} \hat{\mathbf{n}} + t_{\perp} \hat{\mathbf{p}} \quad (4.3)$$

Since the cross product of the parallel component and  $\hat{\mathbf{n}}$  is the zero vector, we require the cross product of the orthogonal component and  $\hat{\mathbf{n}}$  be equal to  $\mathbf{c}$ .

$$t_{\perp} \hat{\mathbf{p}} \times \hat{\mathbf{n}} = \mathbf{c} \quad (4.4)$$

Since  $\mathbf{c}$  and  $\hat{\mathbf{n}}$  are already orthogonal, one of the possible values for the unit vector  $\hat{\mathbf{p}}$  is  $\hat{\mathbf{p}} = \hat{\mathbf{n}} \times \hat{\mathbf{c}}$  (the other possibility is its additive inverse). Note that the unit vector  $\hat{\mathbf{c}}$  is  $\mathbf{c}$  normalized to unit length. Using the vector triple product identity  $\mathbf{a} \times (\mathbf{b} \times \mathbf{c}) = (\mathbf{a} \cdot \mathbf{c})\mathbf{b} - (\mathbf{a} \cdot \mathbf{b})\mathbf{c}$ , it can be showed that

$$\begin{aligned} \hat{\mathbf{p}} \times \hat{\mathbf{n}} &= (\hat{\mathbf{n}} \times \hat{\mathbf{c}}) \times \hat{\mathbf{n}} \\ &= \hat{\mathbf{n}} \times (\hat{\mathbf{c}} \times \hat{\mathbf{n}}) \\ &= (\hat{\mathbf{n}} \cdot \hat{\mathbf{n}})\hat{\mathbf{c}} - (\hat{\mathbf{n}} \cdot \hat{\mathbf{c}})\hat{\mathbf{n}} \\ &= 1\hat{\mathbf{c}} - 0\hat{\mathbf{n}} \\ \hat{\mathbf{p}} \times \hat{\mathbf{n}} &= \hat{\mathbf{c}} \end{aligned} \quad (4.5)$$

Substituting the above expression into Equation 4.4, we arrive at the expression for  $t_{\perp}$ :

$$\begin{aligned} t_{\perp} \hat{\mathbf{p}} \times \hat{\mathbf{n}} &= \mathbf{c} \\ t_{\perp} \hat{\mathbf{c}} &= \mathbf{c} \\ t_{\perp} &= \|\mathbf{c}\| \end{aligned} \tag{4.6}$$

The parallel component of  $\hat{\mathbf{t}}$  does not contribute to the cross product, so theoretically  $t_{\parallel}$  can assume any value and Equation 4.2 will hold true. However, since  $\hat{\mathbf{t}}$  is a unit vector, we require that

$$\begin{aligned} t_{\parallel}^2 + t_{\perp}^2 &= 1 \\ t_{\parallel} &= \pm \sqrt{1 - t_{\perp}^2} \end{aligned}$$

The choice of sign on  $t_{\parallel}$  now depends on the orientation of the incident vector  $\hat{\mathbf{i}}$ . When the incident ray **enters** a surface, the transmitted vector  $\hat{\mathbf{t}}$  will point inwards, away from the normal vector. Conversely, when the incident ray **exits** the surface,  $\hat{\mathbf{t}}$  will point outwards. Therefore,

$$t_{\parallel} = \begin{cases} -\sqrt{1 - t_{\perp}^2} & , \hat{\mathbf{i}} \cdot \hat{\mathbf{n}} < 0 \\ \sqrt{1 - t_{\perp}^2} & , \hat{\mathbf{i}} \cdot \hat{\mathbf{n}} > 0 \end{cases}$$

Therefore, the final form of the transmitted vector  $\hat{\mathbf{t}}$  is

$$\begin{aligned} \hat{\mathbf{t}} &= \|\mathbf{c}\| (\hat{\mathbf{n}} \times \hat{\mathbf{c}}) + \text{sgn}(\hat{\mathbf{i}} \cdot \hat{\mathbf{n}}) \sqrt{1 - \|\mathbf{c}\|^2} \hat{\mathbf{n}} \\ \mathbf{c} &= \frac{n_1}{n_2} (\hat{\mathbf{i}} \times \hat{\mathbf{n}}) \end{aligned} \tag{4.7}$$

There are two special considerations. First, if  $\|\mathbf{c}\| > 1$ , the radical in Equation 4.7 is complex-valued, and no refraction occurs. This phenomenon is known as total internal reflection. Second, if the incident ray is tangent to the surface it intersects with ( $\hat{\mathbf{i}} \cdot \hat{\mathbf{n}} = 0$ ), it neither enters or exits the surface. As a result, there is no refraction or reflection.

## Chapter 5

# Ellipsoidal Coordinates Formulation

Much of the solving algorithms detailed later in this manual utilizes finite volume method to solve for the desired states within a droplet. Since the droplets can deviate from perfect sphericity and each turn into an ellipsoid, the use of an ellipsoidal coordinate system is appropriate. There are many ways to formulate such system; the one used here resembles spherical coordinates, but with a different sketch factor in different semi-axial directions.

$$\mathbf{r}(r, \mu, \varphi) = \begin{bmatrix} x' \\ y' \\ z' \end{bmatrix} = \begin{bmatrix} ar\mu \\ br\sqrt{1-\mu^2} \cos \varphi \\ cr\sqrt{1-\mu^2} \sin \varphi \end{bmatrix}, \quad (5.1)$$

where  $r \in [0, 1]$ ,  $\mu \in [-1, 1]$ , and  $\varphi \in (-\pi, \pi]$  are the coordinate variables. The axes  $x'$ ,  $y'$ , and  $z'$  form a rotated Cartesian grid where  $x'$  points to the semi-major direction,  $y'$  to the semi-middle direction, and  $z'$  to the semi-minor direction. As such, the polar cosine  $\mu$  is always measured from the semi-major axis.

The reverse transformations are

$$r = \sqrt{\left(\frac{x'}{a}\right)^2 + \left(\frac{y'}{b}\right)^2 + \left(\frac{z'}{c}\right)^2} \quad (5.2a)$$

$$\mu = \frac{x'}{ar} \quad (5.2b)$$

$$\varphi = \text{arctan2}\left(\frac{z'}{c}, \frac{y'}{b}\right) \quad (5.2c)$$

The basis vectors are defined as followed

$$\mathbf{e}_r \equiv \frac{\partial \mathbf{r}}{\partial r} = \frac{\mathbf{r}}{r} \quad (5.3a)$$

$$\mathbf{e}_\mu \equiv \frac{\partial \mathbf{r}}{\partial \mu} = \begin{bmatrix} ar \\ -br \frac{\mu}{\sqrt{1-\mu^2}} \cos \varphi \\ -cr \frac{\mu}{\sqrt{1-\mu^2}} \sin \varphi \end{bmatrix} \quad (5.3b)$$

$$\mathbf{e}_\varphi \equiv \frac{\partial \mathbf{r}}{\partial \varphi} = \begin{bmatrix} 0 \\ -br \sqrt{1-\mu^2} \sin \varphi \\ cr \sqrt{1-\mu^2} \cos \varphi \end{bmatrix}. \quad (5.3c)$$

The normalized counterparts are denoted as  $\hat{\mathbf{r}}$ ,  $\hat{\mathbf{\mu}}$ , and  $\hat{\mathbf{\varphi}}$ .

## 5.1 Ellipsoidal cells

On a structured ellipsoidal mesh, a cell that occupies the space between the grid points  $[r_{i-1/2}, r_{i+1/2}] \times [\mu_{j-1/2}, \mu_{j+1/2}] \times [\varphi_{k-1/2}, \varphi_{k+1/2}]$  are given the triple index  $(i, j, k)$ . As is common in finite volume codes, cell boundaries are given half-integer indices, while cell centers have whole-integer indices. A depiction of such a cell is shown in Figure 5.1, with all three basis vectors clearly labeled.

As a result of the stretching of the spherical coordinates, the basis vectors are no longer orthogonal. One consequence of the loss of orthogonality is the normal vector on any of the faces does not coincide with a basis vector. Instead, those normal vectors are given by

$$\mathbf{n}_r = \mathbf{e}_\varphi \times \mathbf{e}_\mu \quad (5.4a)$$

$$\mathbf{n}_\mu = \mathbf{e}_r \times \mathbf{e}_\varphi \quad (5.4b)$$

$$\mathbf{n}_\varphi = \mathbf{e}_\mu \times \mathbf{e}_r. \quad (5.4c)$$

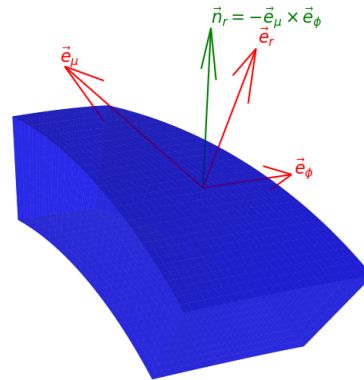


Figure 5.1: A sample ellipsoidal cell

The orientation of each normal vector in Equation 5.4 is chosen such that the dot product between it and corresponding basis vector is positive - i.e. the two vectors both point towards the direction where their respective variable is increasing. Their normalized versions are denoted  $\hat{\mathbf{n}}_r$ ,  $\hat{\mathbf{n}}_\mu$ , and  $\hat{\mathbf{n}}_\varphi$ , respectively. Note that because of degenerate surfaces,  $\hat{\mathbf{n}}_r$  is undetermined at  $r = 0$ , and so is  $\hat{\mathbf{n}}_\varphi$  at  $\mu = \pm 1$ .

The Jacobian determinant indicates how much the volume of this box on  $r$ - $\mu$ - $\varphi$  space is distorted by the transformation onto  $x'$ - $y'$ - $z'$  space.

$$\mathbf{J} = [\mathbf{e}_r \quad \mathbf{e}_\mu \quad \mathbf{e}_\varphi] \quad (5.5a)$$

$$= \begin{bmatrix} a\mu & ar & 0 \\ b\sqrt{1-\mu^2} \cos \varphi & -br \cos \varphi \frac{\mu}{\sqrt{1-\mu^2}} & -br \sqrt{1-\mu^2} \sin \varphi \\ c\sqrt{1-\mu^2} \sin \varphi & -cr \sin \varphi \frac{\mu}{\sqrt{1-\mu^2}} & cr \sqrt{1-\mu^2} \cos \varphi \end{bmatrix} \quad (5.5b)$$

$$dV = |\det \mathbf{J}| dr d\mu d\varphi \quad (5.5c)$$

$$= abcr^2 dr d\mu d\varphi \quad (5.5d)$$

The volume of the cell is then

$$V_{ijk} = \frac{abc}{3} \Delta_i r^3 \Delta_\mu \Delta_\varphi. \quad (5.6)$$

Here, the following short-hand  $\Delta$  notations are employed:

$$\Delta r_i \equiv r_{i+1/2} - r_{i-1/2} \quad (5.7a)$$

$$\Delta_i f(r) \equiv f(r_{i+1/2}) - f(r_{i-1/2}) \quad (5.7b)$$

Most cell have 6 surfaces, each corresponding to a boundary value of  $s$ ,  $\mu$ , or  $\varphi$ , respectively. The exceptions are those with  $r = 0$ , which collapses into a point at the origin, and  $\mu = \pm 1$ , which together form the major axis. The nomenclature for a surface is to add a  $+1/2$  or  $-1/2$  to the index that corresponds to the variable being held constant. For example, surface  $(i + 1/2, j, k)$  is the surface of cell  $(i, j, k)$  where  $r$  is at its maximum value. It is also the surface of cell  $(i + 1, j, k)$  where  $r$  is at its minimum value.

The differential surface area is proportional to the L2-norm of the normal vector. For example, its value on surfaces  $r = r_{i\pm 1/2}$  is

$$dS_{i\pm 1/2, j, k} = \|\mathbf{e}_\mu \times \mathbf{e}_\varphi\|_{r=r_{i\pm 1/2}} d\mu d\varphi \quad (5.8a)$$

$$= \left| \begin{array}{ccc} \hat{\mathbf{i}} & \hat{\mathbf{j}} & \hat{\mathbf{k}} \\ ar_{i\pm 1/2} & -br_{i\pm 1/2} \cos \varphi \frac{\mu}{\sqrt{1-\mu^2}} & -cr_{i\pm 1/2} \sin \varphi \frac{\mu}{\sqrt{1-\mu^2}} \\ 0 & -br_{i\pm 1/2} \sqrt{1-\mu^2} \sin \varphi & cr_{i\pm 1/2} \sqrt{1-\mu^2} \cos \varphi \end{array} \right| d\mu d\varphi \quad (5.8b)$$

$$= r_{i\pm 1/2}^2 \left\| bc\mu \hat{\mathbf{i}} + ac\sqrt{1-\mu^2} \cos \varphi \hat{\mathbf{j}} + ab\sqrt{1-\mu^2} \sin \varphi \hat{\mathbf{k}} \right\| d\mu d\varphi \quad (5.8c)$$

$$= abcr_{i\pm 1/2}^2 \sqrt{\frac{\mu^2}{a^2} + \frac{(1-\mu^2)\cos^2 \varphi}{b^2} + \frac{(1-\mu^2)\sin^2 \varphi}{c^2}} d\mu d\varphi \quad (5.8d)$$

Integrating Equation 5.8d then yields the surface area of surfaces  $(i+1/2, j, k)$

$$\frac{S_{i\pm 1/2,j,k}}{abc} = r_{i\pm 1/2}^2 \int_{\Delta\varphi_k} \int_{\Delta\mu_j} \sqrt{\frac{\mu^2}{a^2} + \frac{(1-\mu^2)\cos^2\varphi}{b^2} + \frac{(1-\mu^2)\sin^2\varphi}{c^2}} d\mu d\varphi \quad (5.9)$$

In Equation 5.9, the  $\varphi$ -dependency of the integrand can be rewritten as two incomplete elliptic integrals of the second kind  $E(\theta, k)$ , as followed:

$$\int_{\Delta\varphi_k} \sqrt{\alpha + \beta \cos^2\varphi + \gamma \sin^2\varphi} d\varphi \quad (5.10a)$$

$$= \int_{\Delta\varphi_k} \sqrt{\alpha + \gamma - (\gamma - \beta) \cos^2\varphi} d\varphi \quad (5.10b)$$

$$= \int_{\pi/2 - \varphi_{k+1/2}}^{\pi/2 - \varphi_{k-1/2}} \sqrt{\alpha + \gamma - (\gamma - \beta) \sin^2\varphi} d\varphi \quad (5.10c)$$

$$= \sqrt{\alpha + \gamma} \int_{\pi/2 - \varphi_{k+1/2}}^{\pi/2 - \varphi_{k-1/2}} \sqrt{1 - \frac{\gamma - \beta}{\alpha + \gamma} \sin^2\varphi} d\varphi \quad (5.10d)$$

$$= \sqrt{\alpha + \gamma} \left[ E\left(\frac{\pi}{2} - \varphi_{k-1/2}, \sqrt{\frac{\gamma - \beta}{\alpha + \gamma}}\right) - E\left(\frac{\pi}{2} - \varphi_{k+1/2}, \sqrt{\frac{\gamma - \beta}{\alpha + \gamma}}\right) \right] \quad (5.10e)$$

$$= -\sqrt{\alpha + \gamma} \Delta_k E\left(\frac{\pi}{2} - \varphi, \sqrt{\frac{\gamma - \beta}{\alpha + \gamma}}\right). \quad (5.10f)$$

Therefore,

$$\frac{S_{i\pm 1/2,j,k}}{ab} = -r_{i\pm 1/2}^2 \int_{\Delta\mu_j} \sqrt{1 - (1 - \epsilon^2)\mu^2} \Delta_k E\left(\frac{\pi}{2} - \varphi, \sqrt{\frac{(1 - \delta^2)(1 - \mu^2)}{1 - (1 - \epsilon^2)\mu^2}}\right) d\mu, \quad (5.11a)$$

where

$$\delta \equiv \frac{c}{b}, \quad (5.11b)$$

$$\epsilon \equiv \frac{c}{a}. \quad (5.11c)$$

The area of the surfaces  $S_{i,j\pm 1/2,k}$  can be calculated similarly

$$\begin{aligned} \frac{S_{i,j\pm 1/2,k}}{ab} &= -\frac{\Delta_i r^2}{2} \sqrt{(1 - \mu_{j\pm 1/2}^2) [\epsilon^2 + (1 - \epsilon^2)\mu_{j\pm 1/2}^2]} \\ &\cdot \Delta_k E\left(\frac{\pi}{2} - \varphi, \sqrt{\frac{\mu_{j\pm 1/2}^2(1 - \delta^2)}{\epsilon^2 + (1 - \epsilon^2)\mu_{j\pm 1/2}^2}}\right), \end{aligned} \quad (5.12)$$

where  $\delta$  and  $\epsilon$  are defined in Equations 5.11b and 5.11c, respectively.

Finally, the area of surfaces  $S_{i,j,k\pm 1/2}$  is

$$\frac{S_{i,j,k\pm 1/2}}{ab} = \frac{\Delta_i r^2}{2} \Delta_j \arcsin(\mu) \sqrt{\delta^2 + (1 - \delta^2) \cos^2 \varphi_{k\pm 1/2}}. \quad (5.13)$$

## 5.2 Del operator

The del operator of a scalar-valued function in ellipsoidal coordinates is

$$\nabla = A_r \mathbf{e}_r + A_\mu \mathbf{e}_\mu + A_\varphi \mathbf{e}_\varphi, \quad (5.14)$$

where the  $A$  factors are found through taking the directional derivative with respect to each of the basis variables.

$$\frac{\partial}{\partial r} = \mathbf{e}_r \cdot \nabla = A_s \mathbf{e}_r \cdot \mathbf{e}_r + A_\mu \mathbf{e}_r \cdot \mathbf{e}_\mu + A_\varphi \mathbf{e}_r \cdot \mathbf{e}_\varphi \quad (5.15a)$$

$$\frac{\partial}{\partial \mu} = \mathbf{e}_\mu \cdot \nabla = A_s \mathbf{e}_\mu \cdot \mathbf{e}_r + A_\mu \mathbf{e}_\mu \cdot \mathbf{e}_\mu + A_\varphi \mathbf{e}_\mu \cdot \mathbf{e}_\varphi \quad (5.15b)$$

$$\frac{\partial}{\partial \varphi} = \mathbf{e}_\varphi \cdot \nabla = A_s \mathbf{e}_\varphi \cdot \mathbf{e}_r + A_\mu \mathbf{e}_\varphi \cdot \mathbf{e}_\mu + A_\varphi \mathbf{e}_\varphi \cdot \mathbf{e}_\varphi, \quad (5.15c)$$

which is equivalent to

$$\begin{bmatrix} A_r \\ A_\mu \\ A_\varphi \end{bmatrix} = \begin{bmatrix} \mathbf{e}_r \cdot \mathbf{e}_r & \mathbf{e}_r \cdot \mathbf{e}_\mu & \mathbf{e}_r \cdot \mathbf{e}_\varphi \\ \mathbf{e}_\mu \cdot \mathbf{e}_r & \mathbf{e}_\mu \cdot \mathbf{e}_\mu & \mathbf{e}_\mu \cdot \mathbf{e}_\varphi \\ \mathbf{e}_\varphi \cdot \mathbf{e}_r & \mathbf{e}_\varphi \cdot \mathbf{e}_\mu & \mathbf{e}_\varphi \cdot \mathbf{e}_\varphi \end{bmatrix}^{-1} \begin{bmatrix} \frac{\partial}{\partial r} \\ \frac{\partial}{\partial \mu} \\ \frac{\partial}{\partial \varphi} \end{bmatrix}. \quad (5.16)$$

In terms of the basis vectors and partial derivatives, Equation 5.14 can therefore be written as

$$\nabla = \underbrace{\begin{bmatrix} \mathbf{e}_r & \mathbf{e}_\mu & \mathbf{e}_\varphi \end{bmatrix}}_{\mathbf{J}} \underbrace{\begin{bmatrix} \mathbf{e}_r \cdot \mathbf{e}_r & \mathbf{e}_r \cdot \mathbf{e}_\mu & \mathbf{e}_r \cdot \mathbf{e}_\varphi \\ \mathbf{e}_\mu \cdot \mathbf{e}_r & \mathbf{e}_\mu \cdot \mathbf{e}_\mu & \mathbf{e}_\mu \cdot \mathbf{e}_\varphi \\ \mathbf{e}_\varphi \cdot \mathbf{e}_r & \mathbf{e}_\varphi \cdot \mathbf{e}_\mu & \mathbf{e}_\varphi \cdot \mathbf{e}_\varphi \end{bmatrix}}_{\mathbf{G}^{-1}}^{-1} \begin{bmatrix} \frac{\partial}{\partial r} \\ \frac{\partial}{\partial \mu} \\ \frac{\partial}{\partial \varphi} \end{bmatrix}. \quad (5.17)$$

The finite volume method presented in this work is second-order, where the gradient on every surface is approximated as constant. The basis vectors  $\mathbf{e}_r$ ,  $\mathbf{e}_\mu$ , and  $\mathbf{e}_\varphi$  that appear in Equation 5.17 are then evaluated at the surface centroid.

The partial derivatives are typically approximated using a central-difference formula; however, the fact that the gradient on any cell surface where a variable is constant includes derivatives in all other variables requires further approximation. For example, take a representative surface  $(i + 1/2, j, k)$  that borders cells  $(i, j, k)$  and  $(i + 1, j, k)$ , as shown in Figure 5.2. The  $r$ -derivative is easily computed directly from the two neighboring cells, assuming each cell-averaged value occurs at the respective cell centroid.

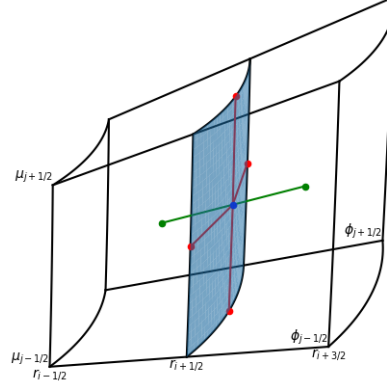


Figure 5.2: The gradient is assumed constant throughout the blue surface ( $i + 1/2, j, k$ ), assuming its value at  $(r_{i+1/2}, \mu_j, \varphi_k)$ , marked in blue. The partial derivative in  $r$  can be evaluated from cell-averaged states, marked in green. The other partial derivatives are evaluated using surface states, marked in red; these values are not explicitly stored and will have to be reconstructed.

$$\frac{\partial u}{\partial r} \Big|_{i+1/2,j,k} \approx \frac{u_{i+1,j,k} - u_{ijk}}{\frac{1}{2}(r_{i+3/2} - r_{i-1/2})}, \quad (5.18)$$

where  $u_{ijk}$  is short-hand for the state variable  $u$  evaluated at point  $(r_i, \mu_j, \varphi_k)$ .

The  $\mu$ -derivative,

$$\frac{\partial u}{\partial \mu} \Big|_{i+1/2,j,k} \approx \frac{u_{i+1/2,j+1/2,k} - u_{i+1/2,j-1/2,k}}{\Delta \mu_j}, \quad (5.19)$$

requires states on the surface  $r = r_{i+1/2}$  rather than cell-averaged states, and therefore not stored. Those values can be reconstructed from the fact that the gradient on that surface,  $\nabla u|_{i+1/2,j,k}$ , has been assumed constant.

$$u_{i+1/2,j+1/2,k} \approx u_{i+1/2,j,k} + \nabla u|_{i+1/2,j,k} \cdot (\mathbf{r}_{i+1/2,j+1/2,k} - \mathbf{r}_{i+1/2,j,k}) \quad (5.20a)$$

$$u_{i+1/2,j-1/2,k} \approx u_{i+1/2,j,k} + \nabla u|_{i+1/2,j,k} \cdot (\mathbf{r}_{i+1/2,j-1/2,k} - \mathbf{r}_{i+1/2,j,k}) \quad (5.20b)$$

Therefore,

$$\frac{\partial u}{\partial \mu} \Big|_{i+1/2,j,k} \approx \frac{\nabla u|_{i+1/2,j,k} \cdot \Delta_j \mathbf{r}_{i+1/2,k}}{\Delta \mu_j}, \quad (5.21)$$

where the short-hand

$$\Delta_j \mathbf{r}_{i+1/2,k} = \mathbf{r}_{i+1/2,j+1/2,k} - \mathbf{r}_{i+1/2,j-1/2,k} \quad (5.22)$$

is used.

Similarly,

$$\frac{\partial u}{\partial \varphi} \Big|_{i+1/2,j,k} \approx \frac{\nabla u|_{i+1/2,j,k} \cdot \Delta_k \mathbf{r}_{i+1/2,j}}{\Delta \varphi_k}. \quad (5.23)$$

Note that in Equation 5.17, the partial derivatives are used to calculate the gradient, while in Equations 5.21 and 5.23, the opposite occurs. This results in the following implicit, yet linear, system of equations to solve for in order to obtain the gradient on surface  $(i + 1/2, j, k)$ :

$$\nabla u = \mathbf{J} \mathbf{G}^{-1} \begin{bmatrix} \frac{2(u_{i+1,j,k} - u_{ijk})}{r_{i+3/2} - r_{i-1/2}} \\ \frac{\nabla u \cdot \Delta_j \mathbf{r}_{i+1/2,k}}{\Delta \mu_j} \\ \frac{\nabla u \cdot \Delta_k \mathbf{r}_{i+1/2,j}}{\Delta \varphi_k} \end{bmatrix}. \quad (5.24)$$

Note that the matrices  $\mathbf{J}$  and  $\mathbf{G}$  in Equation 5.24 are evaluated at  $(r_{i+1/2}, \mu_j, \varphi_k)$ . The gradient on the other surfaces can be computed using similar derivations.

# Chapter 6

## Heat Equation

The general form of the Heat Equation is

$$\frac{\partial}{\partial t} [\rho \hat{H}] = -\nabla \cdot \mathbf{q}'' + q''', \quad (6.1)$$

where

$$\begin{aligned}\rho &:= \text{density (kg/m}^3\text{)} \\ \hat{H} &:= \text{specific enthalpy (J/kg)} \\ \mathbf{q}'' &:= \text{heat flux (W/m}^2\text{)} \\ q''' &:= \text{volumetric heat generation rate (W/m}^3\text{)}\end{aligned}$$

The temperature dependency of the density and specific heat capacity,  $\hat{C}_p$  is assumed to be weak; this is true when the material is a liquid far from phase transition. The time derivative of enthalpy is then approximated in terms of only temperature change:

$$\frac{\partial}{\partial t} [\rho \hat{H}] \approx \rho(T) \hat{C}_p(T) \frac{\partial T}{\partial t} \quad (6.2)$$

Fourier's Law states that the heat flux vector can be written as

$$\mathbf{q}'' = -\nabla[k(T)T] \quad (6.3)$$

Substituting the expressions in Equations 6.2 and 6.3 into the Heat Equation and integrating over a control volume ( $i, j, k$ ), we arrive at the finite-volume discretization

$$\rho_{ijk} \hat{C}_{p,ijk} V_{ijk} \frac{\partial T_{ijk}}{\partial t} = \oint_{\partial V_{ijk}} \nabla[k(T)T] \cdot \hat{\mathbf{n}} dS + q_{ijk}, \quad (6.4)$$

where the quantities with an  $ijk$  subscript are defined as follow

$$V_{ijk} \equiv \iiint_{V_{ijk}} dV \quad (6.5a)$$

$$T_{ijk} \equiv \frac{1}{V_{ijk}} \iiint_{V_{ijk}} T dV \quad (6.5b)$$

$$q_{ijk} \equiv \iiint_{V_{ijk}} q''' dV \quad (6.5c)$$

$$\rho_{ijk} \equiv \rho(T_{ijk}) \quad (6.5d)$$

$$\hat{C}_{p,ijk} \equiv \hat{C}_p(T_{ijk}) \quad (6.5e)$$

As computational domain is inside a droplet that typically assumes an ellipsoidal shape, ellipsoidal coordinates will be used throughout this chapter. The description of this coordinate system can be found in Chapter 5. The following sections aim to expand each term in Equation 6.4 in ellipsoidal coordinates.

## 6.1 Flux term

The gradient of  $kT$  in the flux term on each of the surfaces in cell  $(i,j,k)$  is computing using formulations similar to Equation 5.24. Then the flux integral is simply the sum over all surfaces. Since the gradient on any surface only involves the cell of interest and its neighbor across that surface, the flux term only communicates with up to 6 neighboring cells.

$$\iint_{\partial V_{ijk}} \nabla kT \cdot \hat{\mathbf{n}} dS \approx \sum_{s=1}^{N_{\text{surf}}} [\nabla kT \cdot \hat{\mathbf{n}}]_{ijk,s} S_{ijk,s}. \quad (6.6)$$

Equation 6.6 works well for interior cells. Boundary cells typically have the flux terms for its boundary surfaces modified to account for boundary conditions. Six boundary conditions are required to fully describe the system; however, if the computing domain is a whole ellipsoid, five of them do not need to be specified.

1. The flux terms on the surfaces  $r = 0$  and  $\mu = \pm 1$  are readily omitted. This can be justified by the degenerate surface that collapses at those points.
2. The surfaces  $\varphi = -\pi$  and  $\varphi = \pi$  form a set of periodic boundaries.

The only boundary condition that needs specifying is that at  $r = 1$ , which can be classified as either Dirichlet, Neumann, or Robin. In the following formulation of each boundary condition, function evaluations are almost always done at surface centroid of a boundary cell, i.e. at  $(\mu_j, \varphi_k)$ , so the angular dependencies and the associated subscripts are implicit unless noted otherwise.

### 6.1.1 Dirichlet boundary condition

The boundary condition takes the form

$$T(1) = T^b. \quad (6.7)$$

A layer of ghost cells can be constructed that extends to  $r_{N_r+3/2}$  and prescribed a temperature that averages out to  $T^b$  when combined with the temperature at cell  $N_r$ . The average is just the arithmetic mean of the two temperatures if the ghost cell and its neighboring boundary cell are equivolume. The boundary of such a ghost cell is then

$$r_{N_r+3/2}^3 - 1 = 1 - r_{N_r-1/2}^3 \quad (6.8a)$$

$$r_{N_r+3/2}^3 = \sqrt[3]{2 - r_{N_r-1/2}^3} \quad (6.8b)$$

From there, the partial derivative with respect to  $r$  at  $r = 1$  is

$$\left. \frac{\partial kT}{\partial r} \right|_{N_r+1/2} = 4 \frac{k^b T^b - k T_{N_r}}{\sqrt[3]{2 - r_{N_r-1/2}^3} - r_{N_r-1/2}} \quad (6.9)$$

### 6.1.2 Neumann boundary condition

The boundary condition takes the form

$$\nabla T(1) \cdot \hat{\mathbf{n}}_r(1) = f, \quad (6.10)$$

which directly specifies the flux on the outer surface, but without the thermal conductivity. Assuming  $k$  is evaluated at the cell temperature, the flux term is  $k_{N_r} f$ .

### 6.1.3 Robin boundary condition

The boundary condition takes the form

$$c_1 \nabla T^b \cdot \hat{\mathbf{n}}_r^b + c_0 T^b = f. \quad (6.11)$$

The boundary temperature  $T^b = T$  must be reconstructed from the cell-averaged temperature  $T_{N_r}$ :

$$T^b = T_{N_r} + \nabla T^b \cdot (\mathbf{r}(1) - \mathbf{r}_{N_r}) \quad (6.12)$$

The boundary gradient  $\nabla T^b$  is still an unknown. Using Equation 5.24 for a complete expansion of the gradient, the boundary condition is expressed as

$$c_1 \begin{bmatrix} \frac{T^b - T_{N_r}}{1 - r_{N_r}} \\ \frac{\nabla T^b \cdot \Delta_j \mathbf{r}_{N_r+1/2,k}}{\Delta \mu_j} \\ \frac{\nabla T^b \cdot \Delta_k \mathbf{r}_{N_r+1/2,j}}{\Delta \varphi_k} \end{bmatrix}^T \mathbf{G}^{-1} \begin{bmatrix} \mathbf{e}_r^b \cdot \hat{\mathbf{n}}_r^b \\ 0 \\ 0 \end{bmatrix} + c_0 T^b = f. \quad (6.13)$$

Two more equations are needed to fully specify this system. They are formed by taking the dot product of  $\nabla T^b$  with the remaining two unit normal vectors on the boundary:

$$\nabla T^b \cdot \hat{\mathbf{n}}_\mu^b = \begin{bmatrix} \frac{T^b - T_{N_r}}{1 - r_{N_r}} \\ \frac{\nabla T^b \cdot \Delta_j \mathbf{r}_{N_r+1/2,k}}{\Delta \mu_j} \\ \frac{\nabla T^b \cdot \Delta_k \mathbf{r}_{N_r+1/2,j}}{\Delta \varphi_k} \end{bmatrix}^T \mathbf{G}^{-1} \begin{bmatrix} \mathbf{e}_\mu^b \cdot \hat{\mathbf{n}}_\mu^b \\ 0 \\ 0 \end{bmatrix} \quad (6.14)$$

$$\nabla T^b \cdot \hat{\mathbf{n}}_\phi^b = \begin{bmatrix} \frac{T^b - T_{N_r}}{1 - r_{N_r}} \\ \frac{\nabla T^b \cdot \Delta_j \mathbf{r}_{N_r+1/2,k}}{\Delta \mu_j} \\ \frac{\nabla T^b \cdot \Delta_k \mathbf{r}_{N_r+1/2,j}}{\Delta \varphi_k} \end{bmatrix}^T \mathbf{G}^{-1} \begin{bmatrix} 0 \\ 0 \\ \mathbf{e}_\phi^b \cdot \hat{\mathbf{n}}_\phi^b \end{bmatrix} \quad (6.15)$$

Equations 6.12 through 6.15 form a complete system of equations that can be used to solve for  $T^b$  and  $\nabla T^b$ .

#### 6.1.4 Flux update

Let  $\mathbf{t}$  be a flattened vector of discretized temperature values at each cell. The convention here is  $r\text{-}\mu\text{-}\varphi$  ordering, with  $r$  being the outermost variable and  $\varphi$  being the innermost variable. The corresponding flux vector,  $\mathbf{F}$  can be computed simultaneously for all cells in the form

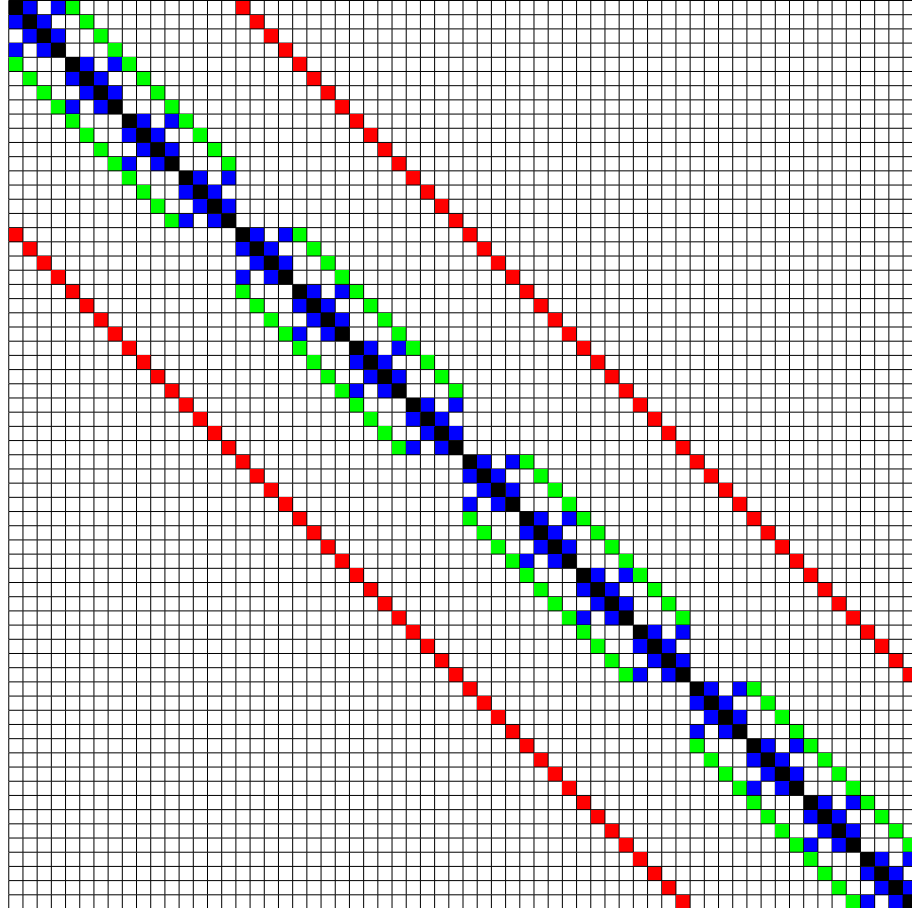
$$\mathbf{f} = \mathbf{D}(\mathbf{t})\mathbf{t} + \mathbf{b}(\mathbf{t}), \quad (6.16)$$

where the diffusion matrix  $\mathbf{D}(\mathbf{t})$  contains the "communications" with neighboring cells, and  $\mathbf{b}$  is the boundary-condition vector. The  $\mathbf{t}$  dependency of  $\mathbf{D}$  and  $\mathbf{b}$  comes from the thermal conductivity. Because each cell only retrieves information from itself and at most 6 neighboring cells to get the flux,  $\mathbf{D}$  is a very sparse matrix (with at most 7 entries on each row). Consider a discretization where each spatial variable is partitioned into 4 intervals,  $\mathbf{D}$  would look like Table 6.1. Moreover,  $\mathbf{D}$  is symmetric and diagonally dominant, making it eligible for a wide range of specialized solvers such as conjugate gradient.

## 6.2 Source term

Finite volume methods blend well with laser heat deposition as the line heat source is easily integrated over each cell the laser passes through. The total energy deposited in any cell is proportional to the amount of intensity attenuated as the laser passes through that cell.

Table 6.1: Full layout of matrix  $\mathbf{D}$  for  $N_r = N_\mu = N_\varphi = 4$ . The diagonal entries are colored black and represent self-communication. Red, green, and blue colored entries indicate neighboring cells in the  $r$ ,  $\mu$ , and  $\varphi$  directions, respectively. Note the periodic nature of  $\varphi$ .



Consider a laser beam that enters an ellipsoidal droplet at position  $\mathbf{r}$  with direction  $\hat{\omega}$ . The vectors are most likely given in standard Cartesian coordinates and will have to be transformed into the rotated system that aligns with the droplet's principal axes. The point of entrance is on the surface  $r = 1$  of cell  $(N_r, j, k)$ , i.e. surface  $(N_r + 1/2, j, k)$ . The surface on which the laser exits the same cell is one that yields the smallest positive distance travel,  $s$ , out of the five remaining surfaces. Computing the distances is therefore the main routine of source term calculations.

For example, the distance  $s$  that the laser travels from surface  $(N_r + 1/2, j, k)$

to  $(N_r - 1/2, j, k)$  is one that satisfies

$$\mathbf{r}(1, \mu_{\text{in}}, \varphi_{\text{in}}) + \hat{\boldsymbol{\omega}} s = \mathbf{r}(r_{N_r - 1/2}, \mu_{\text{out}}, \varphi_{\text{out}}). \quad (6.17)$$

This is a well-determined problem of 3 unknowns -  $s$ ,  $\mu_{\text{out}}$  and  $\varphi_{\text{out}}$ . Because the Jacobian matrix is easily computed

$$\mathbf{J} = [\hat{\boldsymbol{\omega}} \quad -\mathbf{e}_\mu \quad -\mathbf{e}_\varphi], \quad (6.18)$$

Newton's method is the optimal solver candidate. The obtained solution must satisfy

$$s > 0 \quad (6.19a)$$

$$\mu_{j-1/2} \leq \mu_{\text{out}} \leq \mu_{j+1/2} \quad (6.19b)$$

$$\varphi_{k-1/2} \leq \varphi_{\text{out}} \leq \varphi_{k+1/2} \quad (6.19c)$$

in order to be considered.

Similar routines can be carried out to calculate the distance to other surfaces, and the variable held constant on any surface does not have its basis vector appear in the Jacobian. Once the smallest positive  $s$  is found, the amount of energy deposited on cell  $(i, j, k)$  is

$$q_{ijk} = q_{\text{in}}(1 - e^{-\sigma s}), \quad (6.20)$$

where  $\sigma$  is the attenuation coefficient of the droplet.  $q_{\text{in}}$  is updated as  $q_{\text{in}} e^{-\sigma s}$  for the next cell.

The routine terminates once the ray exits surface  $r = 1$ .

### 6.3 Time integration

# Appendix A

## Linear transformation

A linear transformation can be represented by a matrix multiplication. In this project, such matrices are in  $\mathbb{R}^{3 \times 3}$ , meaning they operate on an input on  $\mathbb{R}^3$  to produce an output also on  $\mathbb{R}^3$ . This therefore excludes reduction transformations such as projection. A consequence of this is that the transformation matrix is invertible. Translation is not a linear transformation and therefore cannot be represented by a matrix in  $\mathbb{R}^{3 \times 3}$ . However, it is easy to account for since a mere translation does not change the original shape's orientation or size.

Every shape defined by a user-input function has a shared pointer to a base shape, related to the actual shape by a transformation  $\mathbf{M}$  and a translation vector  $\mathbf{r}_0$ . The transformed shape derived from a parametric surface  $\mathbf{r}(u, v)$  is  $\mathbf{M}\mathbf{r}(u, v) + \mathbf{r}_0$ , while that derived from an implicit surface  $f(\mathbf{r}) = 0$  is  $f(\mathbf{M}^{-1}(\mathbf{r} - \mathbf{r}_0)) = 0$ .

### A.1 Classification of linear transformations

#### A.1.1 Rigid transformation

A rotation by an angle  $\theta$  about a fixed axis  $\hat{\boldsymbol{\omega}}$  is represented by the matrix

$$\mathbf{R}_{\hat{\boldsymbol{\omega}}}(\theta) = \mathbf{I} + \boldsymbol{\Omega} \sin \theta + \boldsymbol{\Omega}^2 (1 - \cos \theta), \quad (\text{A.1})$$

where  $\boldsymbol{\Omega}$  is the anti-symmetric matrix defined as

$$\boldsymbol{\Omega} \equiv \begin{bmatrix} 0 & -\omega_z & \omega_y \\ \omega_z & 0 & -\omega_x \\ -\omega_y & \omega_x & 0 \end{bmatrix}. \quad (\text{A.2})$$

$\mathbf{R}_{\hat{\boldsymbol{\omega}}}$  is an orthogonal matrix ( $\mathbf{R}_{\hat{\boldsymbol{\omega}}} \mathbf{R}_{\hat{\boldsymbol{\omega}}}^T = \mathbf{I}$ ) with unit determinant.

### A.1.2 Reflection

A reflection about the plane that crosses the origin and has unit normal  $\hat{\mathbf{n}}$  is represented by the matrix

$$\mathbf{R}_{\hat{\mathbf{n}}} \equiv \mathbf{I} - 2\hat{\mathbf{n}} \otimes \hat{\mathbf{n}}. \quad (\text{A.3})$$

Similar to  $\mathbf{R}_{\hat{\omega}}$ ,  $\mathbf{R}_{\hat{\mathbf{n}}}$  is orthogonal, but it has a determinant of -1.

### A.1.3 Scaling

A scaling transformation is represented by the diagonal matrix

$$\mathbf{K} \equiv \begin{bmatrix} K_x & 0 & 0 \\ 0 & K_y & 0 \\ 0 & 0 & K_z \end{bmatrix}. \quad (\text{A.4})$$

If  $K_x = K_y = K_z = K$ , the matrix is simplified to

$$\mathbf{K} = K\mathbf{I}, \quad (\text{A.5})$$

and the scaling is said to be uniform.

### A.1.4 Shearing

A shearing transformation is represented by the matrix

$$\Sigma \equiv \begin{bmatrix} 1 & \Sigma_{xy} & \Sigma_{xz} \\ \Sigma_{yx} & 1 & \Sigma_{yz} \\ \Sigma_{zx} & \Sigma_{zy} & 1 \end{bmatrix}. \quad (\text{A.6})$$

## A.2 Singular value decomposition

The motivation of applying the SVD onto  $\mathbf{M}$  is to identify which transformations is  $\mathbf{M}$  composed of. In particular, if they are only a sequence of rotations, reflections, and uniform scalings, then quite a few properties can be easily computed from those of the base shape.

# Bibliography

- [1] David Eberly. *Robust and Error-Free Geometric Computing*. Taylor & Francis Group, LLC, 2020. URL: <https://www.geometrictools.com/Documentation/IntersectionBoxEllipsoid.pdf>.
- [2] Igor Gilitschenski and Uwe D. Hanebeck. “A robust computational test for overlap of two arbitrary-dimensional ellipsoids in fault-detection of Kalman filters”. In: *2012 15th International Conference on Information Fusion*. 2012, pp. 396–401.
- [3] Garry J. Tee. “Surface Area of Ellipsoid Segment”. In: 2005. URL: <https://api.semanticscholar.org/CorpusID:119797279>.